Published in Terra Nova 19, issue 3, 182-188, 2007
which should be used for any reference to this work

Aseismic deformation in the Alps: GPS vs. seismic strain quantification

Christian Sue,[1,2,4] Bastien Delacou,[2] Jean-Daniel Champagnac,[3] Cecile Allanic[2] and Martin Burkhard[2]
[1]*Lausanne University, Lausanne, Switzerland;* [2]*Neuchâtel University, Neuchâtel, Switzerland;* [3]*University of Colorado, Boulder, CO, USA;* [4]*Present address: IUEM, Brest University, Brest, France*

ABSTRACT

Neotectonics of the Western and Central Alps is characterized by ongoing widespread extension in the highest zones of the chain and transcurrent/compressive tectonics at the external limits of the belt. The overall geodetically measured deformations also indicate extension across the Western Alps. There is a good qualitative coherency between seismotectonic and geodetic approaches. Here we attempt to quantify the seismic part of the deformation. The seismic strain is compared to the deformation derived from geodesy. In sub-areas of homogeneous seismic stress/strain, we computed the total seismic moment tensor and related strain tensor. This study provides new quantitative elements about the ongoing geodynamic processes in the alpine belt. The important discrepancies obtained between seismic strains and geodetically-measured deformations raise the issue of aseismic deformation in the Alps, which could be related to elastic loading, creeping and/or a slower ductile-style deformation.

Introduction and tectonic setting

The ongoing tectonics of the Western and Central Alps is characterized by a widespread extensional regime located in the core of the belt and a dominant transcurrent tectonic regime at the outer borders of the chain, with some local compressive areas. This highly contrasted pattern has been well established by several regional studies (e.g. Eva *et al.*, 1997; Sue *et al.*, 1999; Kastrup *et al.*, 2004), and by a large-scale alpine synthesis (Delacou *et al.*, 2004). This last study established the stress and strain patterns in the western and central Alps using a database including 389 focal mechanisms. Extensional directions are radial to the belt in the internal zones and in the whole high-chain of the Alps (namely the 'core' of the belt). This extensional regime extends from eastern Switzerland (Grison area) up to the southernmost tip of the western Alps (Fig. 1), following the arcuate shape of the Western/Central Alps. This extension brought a new major viewpoint on the alpine tectonics, a supposed still active collision belt (e.g. Giglia *et al.*, 1996). Both the topography of the chain (see the 3D low-pass filtered DEM Fig. 1) and the Moho geometry (see the Bouger anomaly map of Masson *et al.*, 1999 and the Moho map of Waldhauser *et al.*, 1998) geographically correlate with neotectonic regime. Areas of over-thickened crust (inner zones of the belt) are characterized by an extensional tectonics whereas local compressional tectonic zones are exactly located along the outer boundaries of the belt characterized by a normal thickness crust. This close correlation between the crustal thickness and the tectonic mode leads Delacou *et al.* (2004) to propose a dynamic model, in which the current tectonics would be mostly controlled by buoyancy forces within the alpine root. This result has been strengthened by 2,5D-numerical modelling (Delacou *et al.*, 2005).

The aim of the present paper is to quantify the seismic strain related to this contrasted tectonic regime, in order (i) to provide a more quantitative information on the seismic energy released in the Alps, (ii) to compare the seismic strain with the current stress maps (Delacou *et al.*, 2004), and (iii) last but not the least, to compare qualitatively and quantitatively the seismic strains with the GPS-measured crustal deformations across the Western Alps (Calais, 1999; Calais *et al.*, 2002; Vigny *et al.*, 2002; Nocquet and Calais, 2003).

Correspondence: Professor Christian Sue, IUEM, Place Copernic, F-29210 Plouzané, France. Tel.: +33 2 98 49 88 91; fax: +33 2 98 49 87 60; e-mail: christian.sue@univ-brest.fr

Distribution of the seismic energy

Instrumental database

To achieve our seismic strain quantification in the Alps, we used the synthesis of focal mechanisms compiled by Delacou *et al.* (2004), which comprises 389 reliable focal solutions covering the alpine realm and adjacent regions. We refer to this paper for the discussion concerning the database parameters. This synthesis includes data previously published in the Alps (Ménard, 1988; Thouvenot, 1996; Eva and Solarino, 1998; Sue *et al.*, 1999; Baroux *et al.*, 2001; Kastrup *et al.*, 2004). The location errors for the older events remain quite large (some km), whereas they drop to around 1 km for the 1990 events (Sue *et al.*, 2002). At the scale of this study, these locational uncertainties are of minor importance. This synthesis concerns the Western (French, Italian) and Central (Swiss) Alps, and includes neighbouring areas such as the Rhine Graben and the Ligurian Sea. However, our analyses and discussion will be restricted to the alpine dynamics hereafter. The magnitudes Ml (local magnitudes) of the earthquakes used in this study range from 1 to 6, with only one magnitude 6 event located in the Ligurian Sea in 1963. The magnitude histogram shows that a majority of earthquakes in the Alps are in the

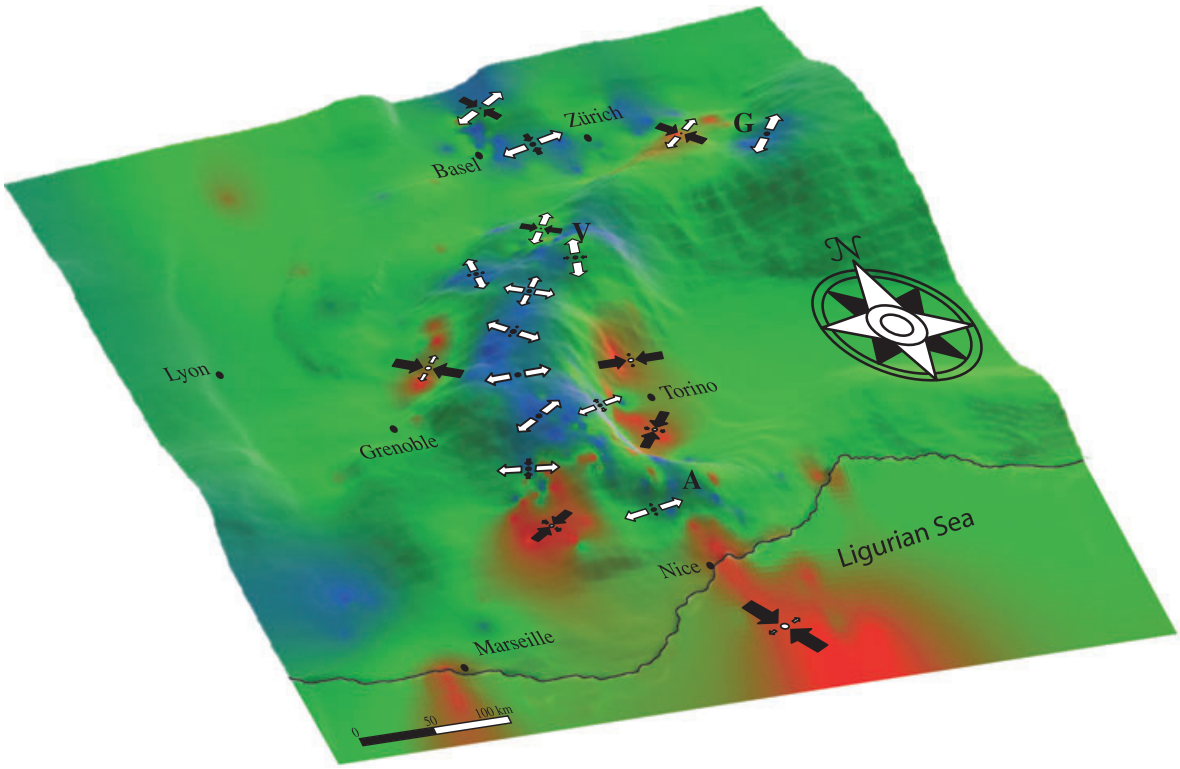

Fig. 1 3D-view of the Western/Central alpine arc looking northeastward, using a 50-km low pass filter applied to the DEM (modified after Delacou *et al.*, 2004). The colour code gives the tectonic mode. Extensional areas (in blue) continuously develop in the high-chain, from the Argentera massif (A) to the Valais area (V), and further to the east in the Grison area (G, eastern Switzerland). They follow the arcuate shape of the belt and are correlated with the overthickened alpine crust. Compressional tectonics is limited to local areas along the border of the alpine orogen (in red). Transcurrent tectonics (in green) concerns the alpine arc as a whole. The arrows give the current stress field ($\sigma 1$ in black, $\sigma 3$ in white).

2–5 range of magnitudes, with only few events reaching magnitude 5 (Fig. 2a). A great jump in technology improved the earthquake's recording at the beginning of the 1990s, which allowed to record most of the events with Ml ≥ 3 in the Alps (e.g. Thouvenot, 1996). Thus, the completeness of the database is fully reliable for the magnitudes range 3–5 after the early 1990s (Fig. 2a,b), although the database regroups events from 1959 to 2000. As we limited our approach to the Alps, this small magnitude-range, combined with the uncertainty we took into account for these magnitudes (see below), allows to compare each of them, despite the long

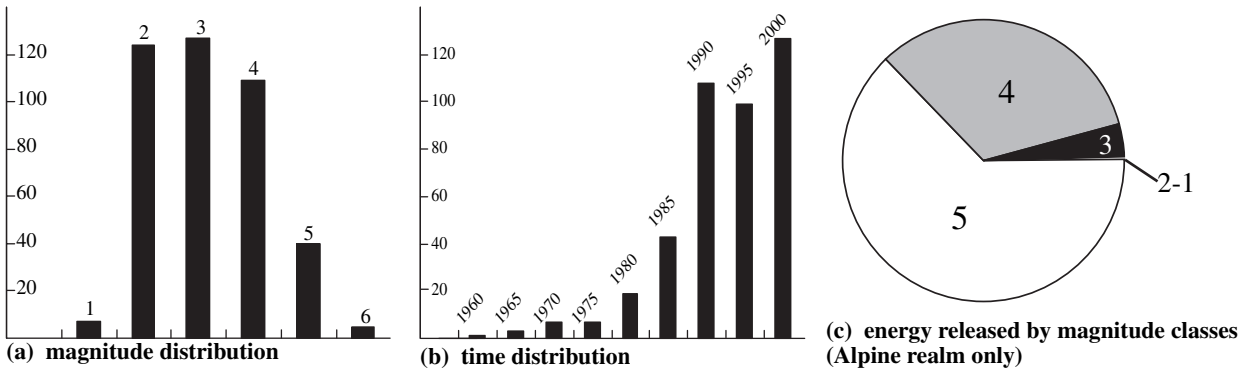

Fig. 2 Magnitude (a), time (b), and energy (c) distribution histograms for the alpine seismicity. The typical magnitude range of the earthquakes in the Alps is 3–5. The completeness of the database appears good in the 1990s. The distribution of the seismic energy in the belt with respect to the magnitude classes shows that the major part of the energy corresponds to magnitude classes 3–5 if we consider only the alpine orogenic system (c). The energy released by the smaller earthquakes (2 and 1) is negligible.

time-window and the use of several catalogues.

Energy vs. magnitude classes

The quantification of the seismic strain in the western Alps is limited by the knowledge of the energy released by earthquakes actually recorded in the belt, and the related uncertainties. Alpine earthquakes are of quite low magnitudes and the available databases have generally been built with short-period instrumentations, which do not allow direct evaluation of the seismic moment. Indeed, we performed such an evaluation using a moment/magnitude relation, and taking into account the uncertainties about the magnitudes and related energy. The scalar seismic moment M0, related to the energy of an earthquake, can be evaluated using a classical relation between magnitude and moment: $\mathrm{Log}(M0) = 1.5\ m + 16.1$ (e.g. Scholz, 1990). This general relationship between magnitudes and moment could be improved for local geodynamic context, but this is far beyond the scope of this paper (Hanks and Kanamori, 1979; Wells and Coppersmith, 1994; Morasca *et al.*, 2005). We used the nominal magnitudes published in the different seismic catalogues compiled by Delacou *et al.* (2004) to evaluate a nominal scalar moment for each event. We are aware of inhomogeneities and uncertainties in the evaluation of low magnitudes among different databases, but the Delacou's synthesis is the best data set currently available on the Alps and one has to deal with these uncertainties.

If we only consider the alpine earthquakes (without the Ligurian Sea and the Rhine Graben, Fig. 2c), around 60% of the global seismic energy is due to magnitude 5 events, around 35% to magnitude 4, some per cents to magnitude 3, and less than 1% to magnitude 2 or lower. From this observation, one can take into account only the 5–3 magnitude range for an evaluation of the seismic strain in the alpine geodynamic context, the energy released by magnitudes 2 and lower being negligible. This also justifies the use of the catalogues available, even if their completeness at small magnitudes is not established.

Mapping of the seismic energy released in the Alps

Figure 3 presents the global pattern of alpine earthquakes used in this study; i.e. those for which a focal mechanism is available. This map displays zones of relative quiescence and others of important activity. Based on the seismic pattern and on our knowledge of alpine tectonics, we divided the belt into several sectors. Each sector is characterized by a tectonic mode and a constant orientation of the stress/stress axis. This zonation is based on the strain/stress maps of Delacou *et al.* (2004) (see Fig. 1 for the tectonic mode and the stress field). We propose a subdivision of the studied area into 14 sectors in the Alpine realm itself (without the Rhine Graben and the Ligurian Sea). The surface area of each sector has been calculated using two characteristic lengths (parallelepipeds, Fig. 3). The maximum depth of brittle deformation, i.e. the seismic activity, has been chosen at 10 km for the 14 sectors (see depth-histogram, insert Fig. 3). Using the volume of each sector, we determined a seismic rate, a seismic yearly-rate, and the

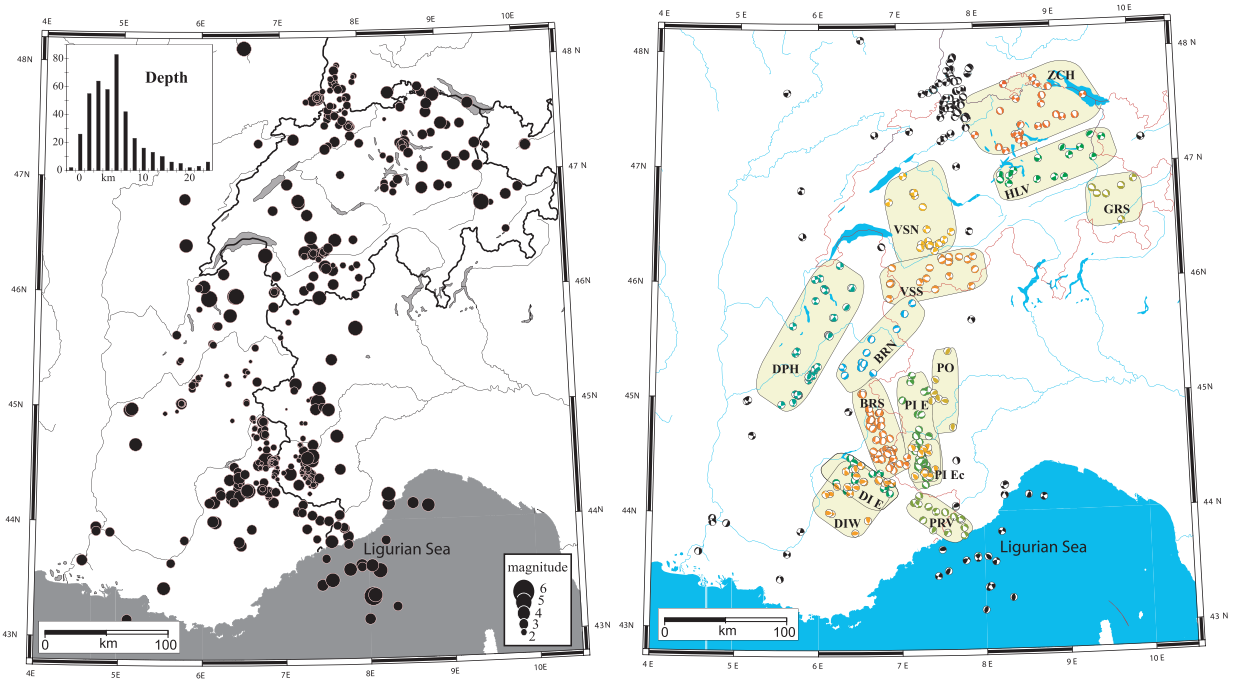

Fig. 3 *Left*: Seismicity map of the earthquakes used in this study. The insert gives the depth distribution of the events, pointing out a typical upper-crustal seismicity in the Alps. *Right*: Map of the focal mechanisms used in this study, showing the 14 sectors used for the seismic strain quantification. The sectors have been individualized using the regionalization of the deformation mode and stress/strain maps in the belt after Delacou *et al.* (2004).

Table 1 Parameters of the scalar moment tensors summed in the 14 sectors.

Zone name	Time (years)	Moment (dyn cm)	Yearly rate (dyn cm yr^{-1})	Volume rate (dyn cm km^3)	yr.vol.rate (dyn cm km^{-3} yr^{-1})
BRN	4	7.01E + 20	1.75E + 20	2.92E + 16	7.30E + 15
BRS	37	1.16E + 24	3.14E + 22	4.30E + 19	1.16E + 18
PIE	25	6.63E + 22	2.65E + 21	2.51E + 18	1.00E + 17
DPH	25	2.36E + 24	9.43E + 22	3.51E + 19	1.40E + 18
VSS	31	3.28E + 23	1.06E + 22	9.10E + 18	2.94E + 17
DIE	11	1.71E + 22	1.55E + 21	6.35E + 17	5.77E + 16
DIW	29	2.30E + 23	7.93E + 21	6.14E + 18	2.12E + 17
HLV	15	6.43E + 22	4.29E + 21	1.54E + 18	1.03E + 17
ZCH	23	6.70E + 22	2.91E + 21	9.31E + 17	4.05E + 16
PIEc	24	1.93E + 23	8.05E + 21	1.94E + 19	8.07E + 17
PO	15	3.21E + 23	2.14E + 22	1.67E + 19	1.12E + 18
PRV	14	8.91E + 21	6.36E + 20	5.62E + 17	4.02E + 16
GRS	13	4.02E + 23	3.09E + 22	3.35E + 19	2.57E + 18
VSN	34	2.34E + 23	6.88E + 21	4.06E + 18	1.19E + 17

'Zone': name of the sector; 'time': duration of the instrumental earthquake recording in the sector; 'moment', 'yearly rate', 'volume rate', 'yr.vol.rate': total sum of the scalar moments, by year, by volume unit, by year and volume unit, respectively.

present in the following the results obtained with a systematic overestimation of 1/2 degree of magnitude, corresponding to a factor 5 of exaggeration for the seismic moment. The resulting size of the strain tensor therefore is an absolute maximum and may be overestimated by a factor of 5 too (linearity between the strain tensor and the moment tensor).

Most of the sectors show very small strain tensors, with some 1/100 mm yr^{-1} of strain for baseline of some 10 km, both for extensional and shortening axes, which is probably not significant (Fig. 4, Table 2). Only the Grison (GRS), Briançonnais (BRS) and Dauphinois (DPH) sectors present larger strains in the 0.1–0.4 mm yr^{-1} range (with baseline in the 30–50 range). In the south-western inner

corresponding yearly volume-rate (Table 1). The yearly rates are affected by the completeness of the catalogues. Although the database is globally complete for the Ml > 3 only for the last 10 years, the information provided by the earthquakes reported before the 1990s can be considered as reliable and must be integrated into our study, as they correspond to the larger shocks that occurred in the belt, and so to major release of seismic energy.

Quantification of the seismic strain

We computed the seismic moment tensors for each sector, by combining the strain information provided by the focal mechanism and the energy/moment information provided by the magnitude (see Kostrov, 1974; Molnar, 1983 for the method). The total moment tensor for a given sector is the sum of all the moment tensors computed for each focal mechanism in this sector. The nominal scalar moments are very low throughout the Alps.

In terms of seismic moment assessment, the relationship we used tends to underestimate the moment for the small magnitudes (Wells and Coppersmith, 1994). It is important to note that there is an increase of a factor 30 in energy/moment for one degree in magnitude. The local magnitudes for the Alps are known with an accuracy of about 1/2 degree. Consequently, we

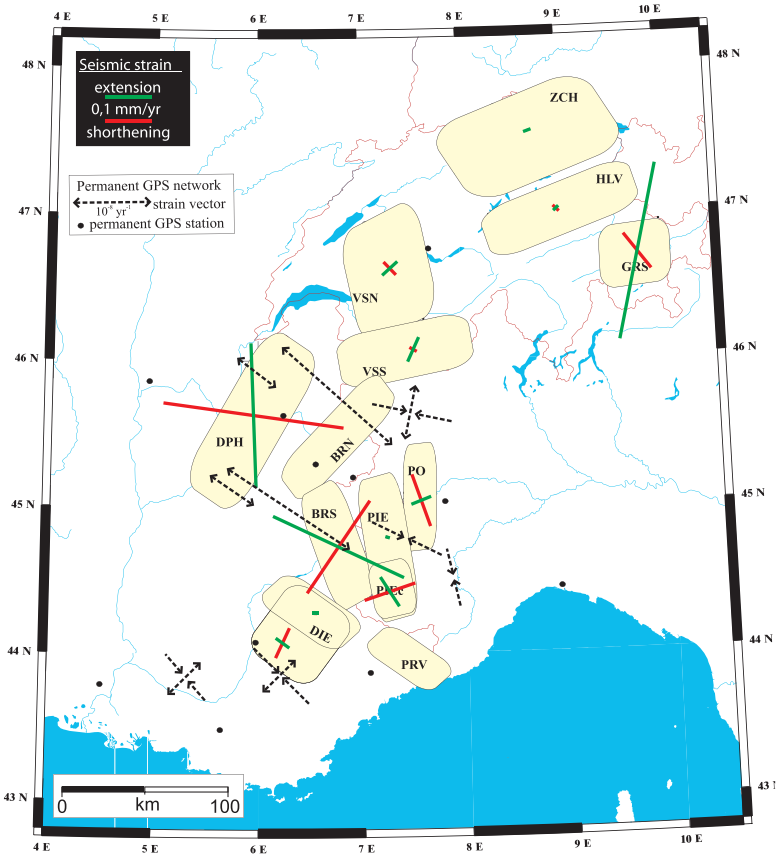

Fig. 4 Map of the seismic strain around the bend of the western/central Alps. The green and red bars give the extensional and shortening axes respectively. Strains are given relatively to the characteristic size of the sectors, i.e. with typical base line of 30–50 km. The dotted black arrows give the deformation measured by the permanent GPS network in the Alps (after Calais *et al.*, 2002). Black dots localize the permanent GPS stations. Note that the Ligurian Sea sector has been voluntarily omitted, because of its marginal position and difference in behaviour with respect to the alpine realm.

Table 2 Parameters of the seismic strain tensors of the 14 sectors.

zone name	P_az (degree)	sh_rate (max, mm yr^{-1})	T_az (degree)	ex_rate (max, mm yr^{-1})
BRN	22	−0.00065	253	0.0008
BRS	34	−0.243	295	0.3125
PIE	15	−0.0064	106	0.01035
DPH	278	−0.3915	178	0.311
VSS	119	−0.01785	24	0.0575
DIE	1	−0.00895	270	0.0153
DIW	25	−0.0715	126	0.0357
HLV	314	−0.0183	46	0.0152
ZCH	135	−0.004015	249	0.0168
PIEc	71	−0.1105	327	0.075
PO	160	−0.1185	68	0.04595
PRV	148	−0.00081	253	0.002765
GRS	321	−0.0965	191	0.386
VSN	136	−0.03835	227	0.04475

'Zone': name of the sector; 'P_az': azimuth of the shortening axis; 'sh_rate': maximized shortening rate (see text for discussion); 'T_az': azimuth of the extensional axis; 'ex_rate': maximized extensional rate.

Alps, the PO, PIEc and DIE sectors also present notable strain tensors, with significant seismic strain. Thus the south-western Alps appear as the area undergoing the main part of the current seismic deformation in the western and central Alps.

Discussion

Seismic strain vs. GPS-related strain

The quantification of seismic strains in the western alpine realm allows further to discuss the ongoing alpine dynamics. First, the low seismic strain we found supports the interpretation that the belt is in a meta-stable state, with low to very low seismic deformation (Sue *et al*., 1999; Sue and Tricart, 2003; Delacou *et al*., 2004). The comparison between GPS-related strain maps of the Alps (Calais *et al*., 2002; Nocquet, 2002; Vigny *et al*., 2002; Nocquet and Calais, 2003) and our seismic strain quantification shows qualitative correlations in terms of mode and direction of deformation. Note that the GPS strains in the Alps generally present large uncertainties, and rarely overstep the 95% ellipsoid error (e.g. Nocquet, 2002). Nevertheless, this is a significant indicator, which supports the use of small earthquakes for such tectonic-related studies (Amelung and King, 1997a; Masson *et al*., 2005). Indeed, the direction of extension in the inner zone of the belt is confirmed by our strain analysis, for instance in the BRS sector, with an extensional rate of 0,3 mm yr^{-1} in a WNW–ESE direction (Sue *et al*., 2000), or in the VSS area (Calais *et al*., 2002; Delacou *et al*., 2004). Some minor differences in axes orientations appear locally (e.g. DPH sector: NW–SE GPS extension, N–S seismic strain extension). Note that our strain tensor for the DPH sector is consistent with dextral transcurrent tectonics, in front of the Belledonne massif (Martinod *et al*., 1996, 2001; Thouvenot *et al*., 2003). The quantitative comparison shows however, that seismic strains are much smaller than the strains deduced from GPS studies. The velocities of 1–2 mm yr^{-1} of extension across the belt deduced from GPS surveys (e.g. Calais *et al*., 2002) must be compared to the 0.1–0.4 mm yr^{-1} we evaluated along comparable baselines. Moreover, these values are found only in some local areas, and taking into account our overestimation of the seismic moment by a factor 5. So, the seismic strain rate accounts at best for a maximum of 10–20% of the geodetic strain rate, within some local areas of the Western Alps. Note that without the overestimation of the moment (using the nominal magnitudes), these proportions are reduced to some per cents. In the other sectors we investigated, the quantitative comparison shows that the seismicity could account for only some per cent to some tenths of per cents of the geodesy-related deformations. The same kind of relationship between GPS-related deformation and seismic strain has already been established in the Alps (Martinod *et al*., 1996; Sue *et al*., 2000; Hinsch and Decker, 2003), at the scale of Europe (Ward, 1998), and in other geodynamic contexts (e.g. Molnar and Deng, 1984; Jackson and McKenzie, 1988; Ekström and England, 1989; Masson *et al*., 2005). Our alpine seismic strain evaluation raises the question of aseismic deformations in the Alps.

Implications in terms of faulting mechanism

These discrepancies between seismic and geodetic strains could be explained first by the lack of large earthquakes in the instrumental period. To go further in this approach, the use of the historical catalogues would be fructuous (e.g. Fäh *et al*., 2003 for Switzerland), but they are sometime difficult to obtain, and they bear far larger uncertainties than the instrumental catalogues in terms of energy. Moreover, no large earthquakes in the historical databases could resume the entire geodetic deformation rates in the Alps. The recurrence time of such large events, in the order of M 6 or higher, could exceed the time-window of historical catalogues in the alpine realm. Such large events have been reported around the belt (e.g. Ligurian Sea; Basel earthquake, Meghraoui *et al*., 2001; Lambesc earthquake, Chardon and Bellier, 2003); however, they could not resume the geodetic strain measured *inside* the Alps. In this interpretation, the deformations measured in the Alps by GPS would be associated with a tectonic loading of elastic energy, which would be released in the future.

A second interpretation implies creeping of the faults (Amelung and King, 1997b). The slow deformations observed in the Alps using geodesy, and the very slow seismic strain rate we computed here, well correspond to this mode of deformation.

A third interpretation implies a more ductile style of deformation, which also could be supported by the slowness of the alpine current tectonics. These processes would be controlled by the relative slowness of the deformation with respect to the rheology of the rocks in the Alps (Sue *et al*., 2002), which may induce a

behaviour close to the brittle/ductile transition (Scholz, 1988, 1990, 1998).

Conclusions

This study brings new quantitative elements on the alpine active tectonics, and allows to compare the geodesy-measured deformations with an evaluation of the seismic strain. Qualitative coherency is established with the strain field measured by GPS concerning the mode and direction of deformation. Quantitatively, maximum 10–20% of the deformation measured by GPS could be explained by the current seismicity, in three sectors. In the other ones, this rate drops to only some per cents. These important discrepancies between seismic strain and geodetic strain raise the issue of aseismic deformation in the Alps, interpreted in terms of elastic loading, creeping, or a brittle/ductile deformation. We propose that aseismic processes (creeping, ductile-style deformation), which could be related to the slowness of the tectonic motions, account for the most part of the current deformation in the Alps.

Acknowledgements

This work was supported by the Neuchâtel and Lausanne Universities, and by the Swiss National Science Found (grants no. 21-61684.00, 200020-101625/1, PBNE2-106764). Many thanks to A. Walpersdorf and F. Masson for fruitful discussions. We owe much to the editor C. Doglioni and to two anonymous reviewers for their constructive comments. Maps were drawn using GMT code (Wessel and Smith, 1991). Special thanks to Ange, Daphné, Mélodie and Ombeline. This paper is dedicated to Martin.

References

Amelung, F. and King, G., 1997a. Large-scale tectonic deformation inferred from small earthquakes. *Nature*, **386**, 702–705.

Amelung, F. and King, G., 1997b. Earthquake scaling laws for creeping and non-creeping faults. *Geophys. Res. Lett.*, **24**, 507–510.

Baroux, E., Béthoux, N. and Bellier, O., 2001. Analyses of the stress field in southeastern France from earthquake focal mechanisms. *Geophys. J. Int.*, **145**, 336–348.

Calais, E., 1999. Crustal deformation in the Western Alps from continuous GPS measurements, 1996–1998. *Geophys. J. Int.*, **38**, 221–230.

Calais, E., Nocquet, J.M., Jouanne, F. and Tardy, M., 2002. Current strain regime in the Western Alps from continuous Global Positioning System measurements, 1996–2001. *Geology*, **30**, 651–654.

Chardon, D. and Bellier, O., 2003. Geological boundary conditions of the 1909 Lambesc (Provence, France) earthquake: structure and evolution of the Trévaresse ridge anticline. *Bull. Soc. Geol. Fr.*, **174**, 497–510.

Delacou, B., Sue, C., Champagnac, J.D. and Burkhard, M., 2004. Present-day geodynamics in the bend of the western and central Alps as constrained by earthquake analysis. *Geophys. J. Int.*, **158**, 753–774.

Delacou, B., Sue, C., Champagnac, J.D. and Burkhard, M., 2005. Origin of the current stress field in the western/central Alps: role of gravitational reequilibration constrained by numerical modelling. In: *Deformation, Rheology and Tectonics: from Minerals to the Lithosphere* (D. Gapais, J.P. Brun and P.R. Cobbold, eds). *Geol. Soc. London Spec. Publ.*, **243**, 295–310.

Ekström, G. and England, P., 1989. Seismic strain rates in regions of distributed continental deformation. *J. Geophys. Res.*, **94**, 10231–10257.

Eva, E. and Solarino, S., 1998. Variations of stress directions in the western Alpine arc. *Geophys. J. Int.*, **135**, 438–448.

Eva, E., Solarino, S., Eva, C. and Neri, G., 1997. Stress tensor orientation derived from fault plane solution in the south-western Alps. *J. Geophys. Res.*, **102**, 8171–8185.

Fäh, D., Giardini, D., Bay, F., Bernardi, F., Braunmiller, J., Deichmann, N., Furrer, M., Gantner, L., Gisler, M., Isenegger, D., Jimenez, M.J., Kästly, P., Koglin, R., Masciadri, V., Rutz, M., Scheidegger, C., Schibler, R., Schorlemmer, D., Schwarz-Zanetti, S., Steimen, S., Sellami, S., Wiemer, S. and Wössner, J., 2003. ECOS and the related macrodeismic database. *Eclogae. Geol. Helv.*, **96**, 219–236.

Giglia, G., Capponi, G., Crispini, L. and Piazza, M., 1996. Dynamics and seismotectonics of the West-Alpine arc. *Tectonophysics*, **267**, 143–175.

Hanks, T.C. and Kanamori, H., 1979. A moment magnitude scale. *J. Geophys. Res.*, **84**, 2348–2350.

Hinsch, R. and Decker, K., 2003. Do seismic slip deficits indicate an underestimated earthquake potential along the Vienna Basin Transfer fault system? *Terra Nova*, **15**, 343–349.

Jackson, J. and McKenzie, D., 1988. The relationship between plate motion and seismic moment tensors, and the rates of active deformation in the Mediterranean and Middle East. *Geophys. J. Roy. Astron. Soc.*, **93**, 45–73.

Kastrup, U., Zoback, M.L., Deichmann, N., Evans, K. and Giardini, D., 2004. Stress field variations in the Swiss Alps and the northern Alpine foreland derived from inversion of fault plane solutions. *J. Geophys. Res.*, **109**, B01402, doi:10.1029/2003JB002550.

Kostrov, B., 1974. Seismic moment and energy of earthquakes and seismic flow of rock. *Izv. Acad. Sci. USSR Phys. Solid Earth*, **1**, 23–40.

Martinod, J., Jouanne, F., Taverna, J., Ménard, G., Gamond, J.F., Darmendrail, X., Notter, J.C. and Basile, C., 1996. Present-day deformation of the Dauphine (SE France) Alpine and Subalpine massifs. *Geophys. J. Int.*, **127**, 189–200.

Martinod, J., Roux, L., Gamond, J.F. and Glot, J.P., 2001. Present-day deformation of the Belledonne Massif (External Alps, France): comparison triangulation-GPS. *Bull. Soc. Geol. Fr.*, **172**, 713–721.

Masson, F., Verdun, J., Bayer, R. and Debeglia, N., 1999. Une nouvelle carte gravimétrique des Alpes occidentales et ses conséquences structurales et tectoniques. *C. R. Acad. Sci. Paris*, **329**, 865–871.

Masson, F., Chéry, J., Hatzfeld, D., Martinod, J., Vernant, P., Tavakoli, F. and Ghafory-Ashtiani, M., 2005. Seismic versus aseismic deformation in Iran inferred from earthquakes and geodetic data. *Geophys. J. Int.*, **160**, 217–226.

Meghraoui, M., Delouis, B., Ferry, M., Giardini, D., Huggenberger, P., Spottke, I. and Granet, M., 2001. Active normal faulting in the Upper Rhine Graben and paleoseismic identification of the 1356 Basel earthquake. *Science*, **293**, 2070–2073.

Ménard, G., 1988. *Structure et cinématique d'une chaîne de collision: Les Alpes occidentales et centrales*. PhD, Thèse de Doctorat d'état, Université Joseph Fourier, 278 pp.

Molnar, P., 1983. Average regional strain due to slip on numerous faults of different orientations. *J. Geophys. Res.*, **88**, 6430–6432.

Molnar, P. and Deng, Q.D., 1984. Faulting associated with larges earthquakes and the average rate of deformation in central and eastern Asia. *J. Geophys. Res.*, **89**, 6203–6228.

Morasca, P., Mayeda, K., Malagnini, L. and Walter, W.R., 2005. Coda-derived source spectra, moment magnitudes and energy-moment scaling in the western Alps. *Geophys. J. Int.*, **160**, 263–275.

Nocquet, J.-M., 2002. *Mesure de la déformation crustale en Europe occidentale par Géodésie spatiale*. PhD thesis, Université de Nice, 307 pp.

Nocquet, J.M. and Calais, E., 2003. Crustal velocity field of western Europe from permanent GPS array solutions, 1996–2001. *Geophys. J. Int*., **154**, 72–88.

Scholz, C.H., 1988. The brittle-plastic transition and the depth of seismic faulting. *Geol. Rundsch*., **77**, 319–328.

Scholz, C.H., 1990. *Mechanics of Earthquakes and Faulting*. Cambridge University Press, Cambridge.

Scholz, C.H., 1998. Earthquakes and friction laws. *Nature*, **391**, 37–42.

Sue, C. and Tricart, P., 2003. Neogene to current normal faulting in the inner western Alps: a major evolution of the late alpine tectonics. *Tectonics*, **22**, 1050, doi: 10.1029/2002TC001426.

Sue, C., Thouvenot, F., Frechet, J. and Tricart, P., 1999. Widespread extension in the core of the western Alps revealed by earthquake analysis. *J. Geophys. Res*., **104**, 25611–25622.

Sue, C., Martinod, J., Tricart, P., Thouvenot, F., Gamond, J.F., Frechet, J., Marinier, D., Glot, J.P. and Grasso, J.R., 2000. Active deformation in the inner western Alps inferred from comparison between 1972-classical and 1996-GPS geodetic surveys. *Tectonophysics*, **320**, 17–29.

Sue, C., Grasso, J.R., Lahaie, F. and Amitrano, D., 2002. Mechanical behavior of western Alpine structures inferred from statistical analysis of seismicity. *Geophys. Res. Lett*., **29**, 65–69.

Thouvenot, F., 1996. *Aspects géophysiques et structuraux des Alpes occidentales et de trois autres orogénèses (Atlas, Pyrénées, Oural)*. PhD, These de doctorat d'Etat, Universite Joseph Fourier, 378 pp.

Thouvenot, F., Frechet, J., Jenatton, L. and Gamond, J.F., 2003. The Belledonne Border Fault: identification of active seismic strike–slip fault in the western Alps. *Geophys. J. Int*., **155**, 174–192.

Vigny, C., Chery, J., Duquesnoy, T., Jouanne, F., Ammann, J., Anzidei, M., Avouac, J.P., Barlier, F., Bayer, R., Briole, P., Calais, E., Cotton, F., Duquenne, F., Feigl, K.L., Ferhat, G., Flouzat, M., Gamond, J.F., Geiger, A., Harmel, A., Kasser, M., Laplanche, M., Le Pape, M., Martinod, J., Menard, G., Meyer, B., Ruegg, J.C., Scheubel, J.M., Scotti, O. and Vidal, G., 2002. GPS network monitors the Western Alps deformation over a five-year period: 1993–1998. *J. Geodesy*, **76**, 63–76.

Waldhauser, F., Kissling, E., Ansorge, J. and Mueller, S., 1998. Three-dimensional interface modelling with two-dimensional seismic data: the Alpine crust-mantle boundary. *Geophys. J. Int*., **135**, 264–278.

Ward, S.N., 1998. On the consistency of earthquake moment release and space geodetic strain rates: Europe. *Geophys. J. Int*., **135**, 1011–1018.

Wells, D.L. and Coppersmith, K.J., 1994. New empirical relationships among magnitude, rupture width, rupture area, and surface displacement. *Bull. Seismol. Soc. Am*., **88**, 635–652.

Wessel, P. and Smith, W.H., 1991. Free software helps map and display data. *EOS Trans. Am. Geophys. Union*, **72**, 441 and 445–446.